UNIVERSITY of York

This is a repository copy of *Phase Transitions in Benzene under Dynamic and Static compression*.

White Rose Research Online URL for this paper:
https://eprints.whiterose.ac.uk/168093/

Version: Accepted Version

**Article:**
Rao, Usha, Chaurasia, S., Mishra, Ajay K. et al. (1 more author) (2020) Phase Transitions in Benzene under Dynamic and Static compression. JOURNAL OF RAMAN SPECTROSCOPY. ISSN 0377-0486

https://doi.org/10.1002/jrs.6047

**Reuse**
Items deposited in White Rose Research Online are protected by copyright, with all rights reserved unless indicated otherwise. They may be downloaded and/or printed for private study, or other acts as permitted by national copyright laws. The publisher or other rights holders may allow further reproduction and re-use of the full text version. This is indicated by the licence information on the White Rose Research Online record for the item.

**Takedown**
If you consider content in White Rose Research Online to be in breach of UK law, please notify us by emailing eprints@whiterose.ac.uk including the URL of the record and the reason for the withdrawal request.

White Rose university consortium
Universities of Leeds, Sheffield & York

eprints@whiterose.ac.uk
https://eprints.whiterose.ac.uk/


# Phase Transitions in Benzene under Dynamic and Static compression

| | |
|---|---|
| Journal: | *Journal of Raman Spectroscopy* |
| Manuscript ID | JRS-20-0208.R1 |
| Wiley - Manuscript type: | Research Article |
| Date Submitted by the Author: | 29-Oct-2020 |
| Complete List of Authors: | Rao, Usha; Bhabha Atomic Research Centre, high pressure and synchrotron radiation physics division<br>Chaurasia, Shivanand; Bhabha Atomic Research Centre, High Pressure & Synchrotron RadiationPhysics Division<br>Mishra, Ajay; Bhabha Atomic Research Centre, High Pressure & synchrotron Radiation Physics Division<br>Pasley, John; University of York, York Plasma Institute, Department of Physics |
| Keywords: | Laser- driven shock, Time-Resolved Raman spectroscopy, High pressure, Static compression |
| | |

SCHOLARONE™
Manuscripts

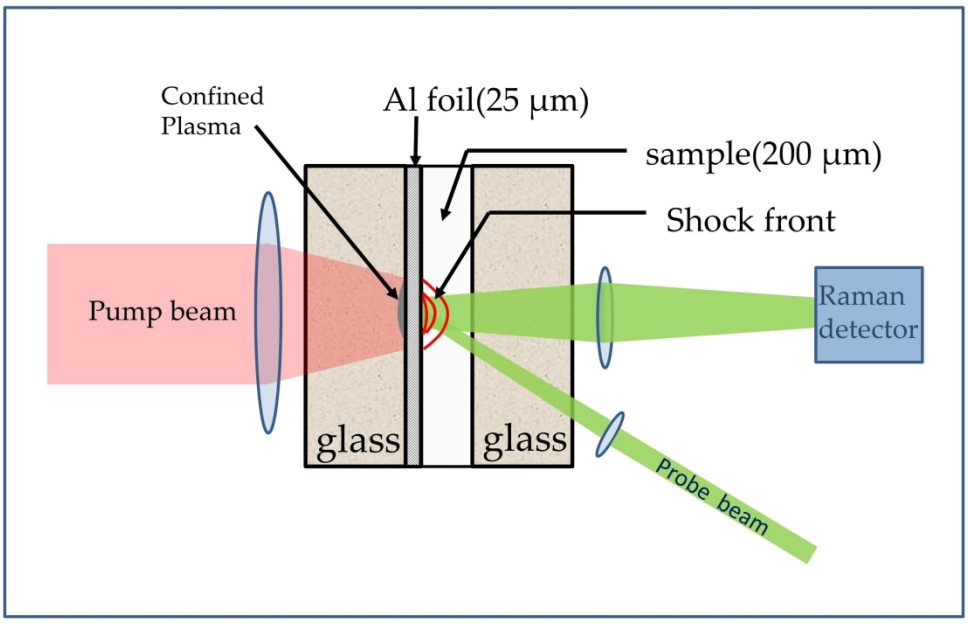


Fig 1. Schematic of pump-probe arrangement for the time resolved Raman spectroscopy of shocked medium. Pump beam hit the target at normal, however, the probe beam hits at 450 which enable the efficient collection of scattered Raman signal.

253x190mm (300 x 300 DPI)

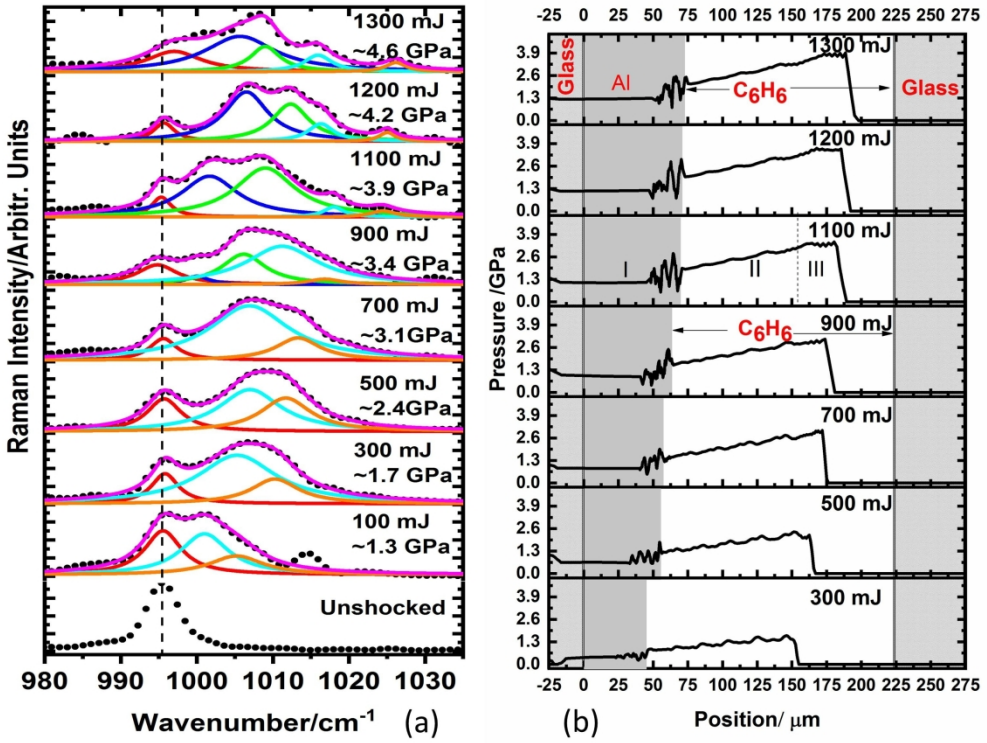


Fig 2a. Lorentzian fit of shocked v1 (993 cm-1) C-C ring breathing mode for different pressures (or laser energies), b. Pressure profile at different laser energies for at 52 ns relative to the start of the pump pulse.

253x190mm (300 x 300 DPI)

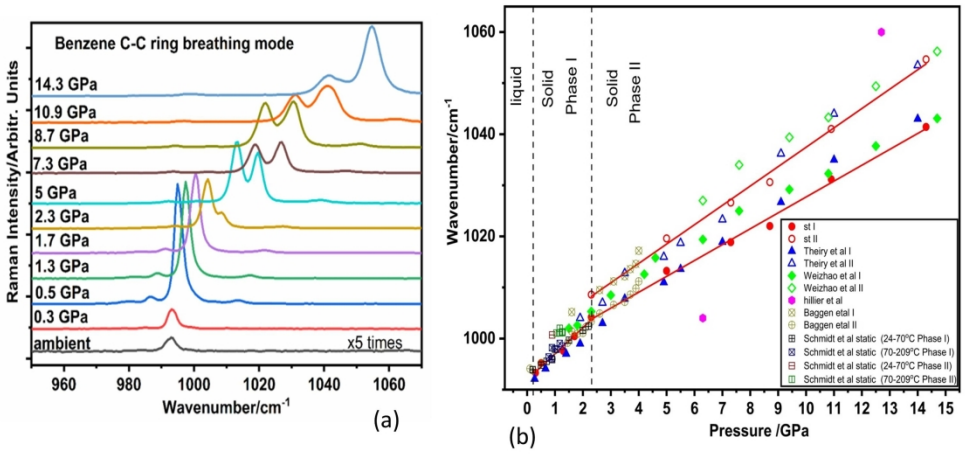


Fig 3(a). Stacked plot of Raman spectra of the C-C ring breathing mode (□1) of benzene (993 cm-1) under Static compression at different pressures. Spectra at ambient is scaled five times. (b) Data from our static pressure measurements are shown as closed and open red circle for Phase -I and phase-II respectively. St-I and St -II indicates the Raman modes in Phase I and II under static compression. Red lines are linear fit to the data for guiding eyes. For other's data, I & II marked against their name are correspond to phase-I and phase-II.

253x190mm (300 x 300 DPI)

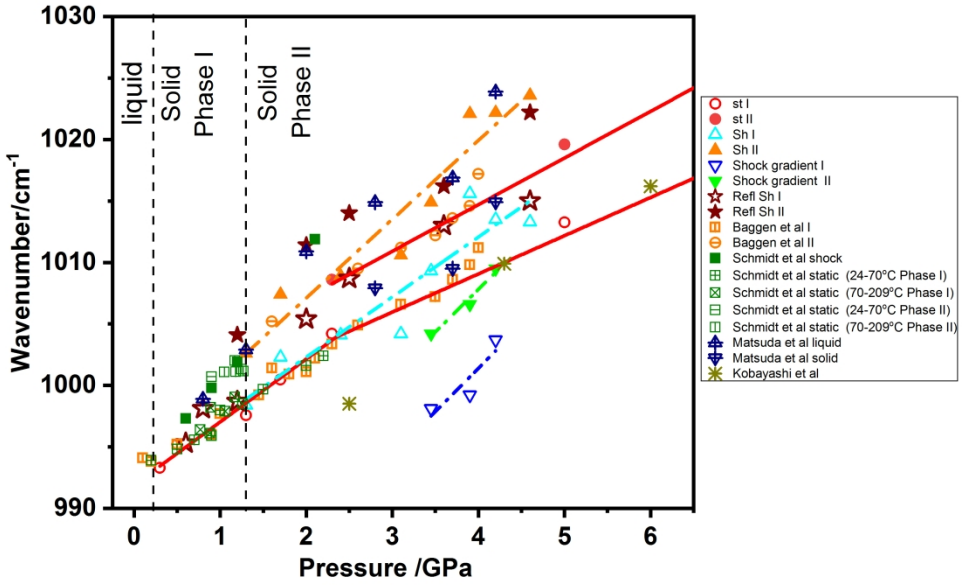


Fig 4 Comparison of Raman shift obtained under shock and static compression (Solid lines are a linear fit to the static compression data; dotted lines are a fit to the shock compression data). St-I, St-II and Sh-I, Sh-II represents data points of the present work corresponds to the Benzene-I and Benzene-II measured in static and dynamic (Shock) experiments respectively. Shock gradient I and Shock Gradient II represents the two new modes from gradient region II. Ref Sh I and Ref Sh II represent the mode shift due to reflected shock wave in the present studies. Works from other authors in Benzene phase I and benzene phase II are represented by I and II in front of the author names.

304x208mm (300 x 300 DPI)

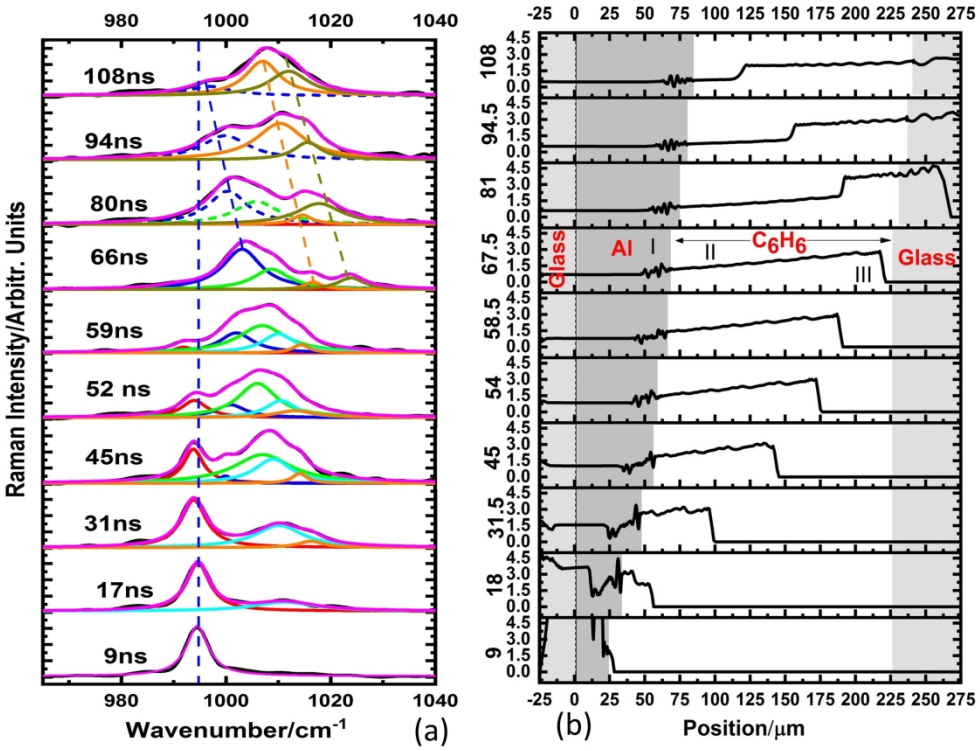


Fig 5a Lorentzian fit of shocked v1 (992 cm-1) C-C ring stretching mode for different delay times, b. Spatial profile of Shock wave at different delay times for laser energy of 700 mJ obtained from one dimensional hydrodynamic simulations

253x190mm (300 x 300 DPI)

# Phase Transitions in Benzene under Dynamic and Static compression

**Usha Rao[1, 2], S. Chaurasia*[1, 3], Ajay K. Mishra[1, 3], John Pasley[4]**

[1] *High Pressure and Synchrotron Radiation Physics Division, Bhabha Atomic Research Centre, Mumbai-400085, India*

[2]*University of Mumbai, Mumbai-400032, India*

[3]*HomiBhabha National Institute, Mumbai-400094, India*

[4]*York Plasma Institute, Department of Physics, University of York, York, YO10 5DQ, UK*

***shibu@barc.gov.in**

For Peer Review

## Abstract:

Phase transitions in liquid Benzene under laser shocked conditions are studied using high resolution time resolved Raman spectroscopic technique. The C-C Ring breathing mode ($\upsilon_1$) of Benzene at 993 $cm^{-1}$ is analyzed to monitor the phase transitions occurring in the Raman spectra during shock wave propagation in the pressure range 1.3 - 5 GPa. Phase transition from Liquid Benzene to solid Benzene (Phase-I) is observed below 1.3 GPa and above this pressure another phase transition from phase-I to Phase-II occurs. We also performed, Raman spectroscopic measurements under static compression employing diamond anvil cell (DAC) to compare the effect of shock wave on Benzene compared to isothermal compression using DAC. In static pressure measurements, the first phase transition from liquid to solid benzene (orthorhombic) occurs at 0.3 GPa and second phase transition from benzene –I (orthorhombic) to Benzene phase -II (monoclinic) occurs at 2.3 GPa, which is higher than that observed in case of shock compression experiments. The observed high-resolution spectrum enables us to determine the effect of pressure gradient upon the Raman spectrum of benzene in shocked condition. One dimensional radiation-hydrodynamic simulations were performed to corroborate the Raman spectroscopic results under dynamic compression. Simulated spatial profiles of the shock wave propagation in benzene at different delay times are used to explain the observation of multiple Raman modes in the spectral region 990-1020 $cm^{-1}$. It is understood that different regions of the sample experience distinct pressure due to shock pressure gradient across the sample. The new Raman modes appearing in this spectral region are attributed to the Raman signals due to phase transition and from differently shocked regions of benzene under dynamic compression. Effect of reflected shock wave from benzene-glass interface manifested

in terms of red shifting and intensity enhancement of Raman modes at higher pressure is explained in this study.

**Keywords:** Laser- driven shock, Time-Resolved Raman spectroscopy, High pressure, Static compression.

## Introduction:

A material under dynamic compression is subjected to a unique and concomitant condition of large compression, high temperature and large deformation which exists for very short time scales causing it to undergo various physical-chemical changes.[1-3] Understanding the material's response under these extreme conditions is of paramount importance for fundamental science. These experiments also provide insights into impact processes relevant to early planetary formation and their evolution.[4, 5] Benzene is found in the atmosphere of Jupiter and is one of the primary sources of carbon.[6] Studies of dynamically shocked benzene can assist in the understanding of many astrophysical phenomena occurring at high pressure and high temperature. Small molecular materials play an essential role in shock compression science since almost all useful explosives are molecular solids.[7-9] Many explosive materials are derivatives of benzene, such as nitrobenzene, DNT, TNT, TATB etc., [10-12] which on detonation have similar behaviour. Therefore, the studies of benzene under extreme conditions (high pressure & high temperature) are of substantial importance for basic research as well as from an application point of view. Benzene is present in significant amount in petroleum, in fuels and is a primary intermediate product formed during combustion of higher aromatics. The high temperature chemistry of benzene plays a significant role in the formation of larger polycyclic aromatic hydrocarbon (PAH) molecules. [13] The distinctive planar molecular structures together with the delocalized π-electron of aromatic compounds make their behaviour under high pressure an important subject for investigation. The delocalized π-electrons of benzene make it extremely stable at ambient conditions, however they are sensitive to compression. Under compression overlapping of neighboring π-orbitals can cause chemical reactions to occur. Hence, understanding the response of benzene molecules under high pressure gives insights into the formation of many complex π-bonded molecules. Recently, new techniques developed for dynamic compression using pulsed-power systems and high-power lasers have made it possible to study the compressive behaviour on timescales as short as tens of femtoseconds, and such experiments often achieve substantially higher pressures

For Peer Review

than earlier gas-gun-based loading techniques.[14] Combining ultrafast time-resolved molecular spectroscopy with the shock compression technique helps with the investigation of the dynamical properties of materials at molecular level. Time-resolved studies of shock-induced phenomena are extremely challenging due to the short time scales involved and the potentially destructive nature of the experiments. Recent advances in instrumentation and techniques for shock-wave spectroscopy, primarily motivated by the study of energetic materials, have led to the development of new methods that can be used to study a wide range of condensed-matter systems.[15] Time resolved spectroscopic methods provide the necessary macroscopic and microscopic insights for the decomposition mechanisms and phase transitions occurring under shock loading. Time-resolved Raman spectroscopy (TRRS), in particular, serves as a direct *in situ* probe which is sensitive to both the chemical and structural changes occurring under shock loading. During the past years a few studies have been done using TRRS on solid and liquid samples. Matsuda and Nakamura have studied the response of benzene and its derivatives, and the response of PTFE, using laser-driven shock compression and TRRS.[16,17] At room temperature, liquid benzene readily crystallizes to phase I at 0.07 GPa in an orthorhombic structure with four molecules per unit cell. Phase II exists between 1.4 and 4 GPa and exhibits a monoclinic structure. Akella and Kennedy constructed a phase diagram of benzene up to 3.5 GPa using the Differential Thermal Analysis (DTA) technique.[18] Ellenson and Nicol performed the low temperature Raman spectroscopy of crystalline Benzene up to a pressure of 4 GPa [19]; they reported the Raman spectra of phase I and phase II of benzene at 77 K. Adams and Appleby measured Raman, infrared and far infrared spectra using Diamond Anvil cell and found anomalies in their spectra at about 3.5 GPa, indicative of a sluggish phase transition from phase II to Phase III.[20] The mid infrared studies below 10 GPa by Anderson et al. [21], further confirmed the I-II and II-III phase transitions. Medina and Shea obtained Brillouin spectra from liquid benzene at temperature ranging from 298 to 349 K at pressure up to 0.3 GPa and deduced from their hypersonic velocity data that complete vibrational relaxation takes place at high pressure.[22] Thiery and Leger investigated crystalline benzene under static compressions up to 25 GPa at room temperature using Raman spectroscopy and powder x-ray diffraction (PXRD) techniques.[23] They observed two first order phase transitions at 1.4 and 4 GPa followed by a second order phase transition at 11 GPa. Chervin [24] using their low temperature Micro-Raman investigated the low temperature phase diagram and temperature induced chemical transformation of benzene. Zhou et al. [25] studied the absolute Raman intensity change with pressure up to 13 GPa and investigated the behavior of inter and intra molecular π - π and C-H π interactions. Xu et al.[26] reported high pressure Micro-Raman spectroscopy





For Peer Review

results up to 15 GPa using high throughput, high sensitivity Raman Notch filter setup and observed benzene II-III and III-III' phase transition. Podsiadlo et al.[27] compared the molecular aggregation of pyridine and pyridazine with that of benzene in its phase I and II and found that benzene remains more stable than pyridine and pyridazine under high pressure. Budzianowski and Katrusiak performed X-ray diffraction studies determining the crystal structure of phase I and found that the changes of molecular arrangement within phase I on elevating the pressure and lowering the temperature are analogous.[28] Ciabini et al.[29,30] performed Infrared spectroscopic studies of Benzene up to 25 GPa under static compression and reported a phase transition between phase III and III' at 11.2 GPa and between phase III' and IV at 17.4 GPa. Pravica et al.[31] performed X-ray Raman studies using DAC up to 20 GPa and suggested polymerization or dimerization of benzene under high pressure. Pruzan et al.[32] reported infrared analysis of benzene in DAC upto a pressure of 30 GPa .They observed chemical transformation of benzene involving a ring opening reaction. Katrusiak et al.[33] performed single crystal X-ray diffraction studies in the pressure range 0.1 MPa to 5 GPa and in the temperature range 295 K to 670 K and have determined the structure of benzene phase II. Recently, Weizhao et al.[34] used high-pressure synchrotron X-ray, neutron diffraction, and micro-Raman spectroscopy together with density functional calculations to investigate the isotope effects in benzene isotopologues $C_6H_6$ and $C_6D_6$ up to 46.0 GPa.

Extensive studies have been performed under high pressure and temperature conditions in benzene under static compression using DAC. However, experiments on dynamically compressed Benzene are still rare due to their complexity. Schmidt et.al.[35], and Kobayashi and Sekine [36] have reported Raman spectra of liquid benzene under shock compression at pressures of 1.2 GPa and 6 GPa respectively using gas and powder guns. Matsuda et.al.,[16] Studied the Raman spectra of benzene under laser-driven shock compression up to 1.3 GPa and observed a pressure induced frequency shift similar to that of Schmidt et al. Seth and Root [37] performed Time Resolved Raman spectroscopy measurements under shock wave conditions utilizing stepwise loading in pressure range between 4 and 25 GPa and have examined high pressure response of liquid benzene at thermodynamic conditions not attainable in single shock compression. Their Raman measurements at 24.5 GPa showed increased background indicating a possible chemical change at this pressure.

In earlier studies on shocked Benzene, experiments with high resolution could not be done due to very small signal throughput in ultrashort (1-3 ns) recording time. Hence, the effect of the pressure gradient in sample could not be unambiguously observed. In this manuscript, we report high-resolution time-resolved Raman spectroscopic studies of Benzene under laser-



For Peer Review

driven shock compression at different time snaps after the incidence of laser beam on the Aluminium foil used for shock generator and with varying laser energies (and hence pressures) at a fixed delay between pump and probe beam. The observed effect of the pressure gradient existing inside the sample during shock-loading on the Raman modes is interpreted with the help of 1D radiation-hydrodynamic simulations using a Lagrangian radiation-hydrodynamics simulation code. We have also performed Raman spectroscopy of Benzene under static compression and have compared the effect of shock-loading (i.e., Hugoniot) with isothermal compression.

## Methods:

### A: Shock Wave Experiments

Nanosecond time-resolved Raman spectroscopy using a pump-probe technique was performed with a 2J/7 ns Nd: YAG laser. A pump beam at 1064 nm was used to drive a shock wave in Aluminium in a confined ablation mode and second-harmonic beam at 532 nm from the same source was used for Raman excitation. The delay between the pump and the probe was adjusted by changing the optical path between two plane mirrors, by changing the number of round trips of the probe beam between the mirrors. Detailed information is described elsewhere.[38] The delay time t = 0 ns between pump and probe is taken as the time when both beams hit Aluminum-glass interface simultaneously. In this experiment a maximum delay of 108 ns between pump and probe has been used. This delay is good enough to record the changes occurred during the shock wave propagation in 200 μm thick sample. This delay time is even enough to record the influence of the reflected shock at late times from the Benzene-glass interface. Benzene is used in the confined target geometry, confined at one end by the Al pusher and at the other by glass. The target assembly consists of a 2.5 mm thick glass window of 2 cm diameter behind which an Aluminium foil of thickness 25 μm is glued. This front portion of the target is separated from the rear portion by a Teflon spacer (200 μm thick) connected to a second layer of glass (2.5 mm thick). The 200 μm void created by the spacer, between the Aluminium foil, and the rear glass layer is then filled with Benzene as shown in figure 1. The target assembly is finally mounted on a motorized X-Y-Z translational stage which was synchronized with the laser system so that each laser pulse hit the fresh sample surface. The fundamental beam was focused to a spot size of 1.8 mm on the Aluminium-glass interface and the probe beam was directed to a matching position from the rear side of the target, with to a beam diameter of 500 μm, so as to probe the most planar region of shock. In the present study

For Peer Review

two types of experiments were performed. In the first set of experiments, the energy of the pump and probe beams were fixed to 700 mJ and 2.5 mJ respectively and the delay between the pump and probe was varied for time resolved studies. In the second set of experiments, the delay between the pump and the probe was fixed at 52 ns and the laser energy of the pump beam (and hence pressure) was varied from 100 mJ to 1300 mJ (approximately 1.3 GPa to 4.6 GPa). Experiments were performed with a resolution of 1 $cm^{-1}$ using the 2400 lines/mm grating of the Andor Shamrock spectrometer and 2 ns ICCD gating. Schematic of the experimental setup is shown in figure S1 (Supporting Information). Further details of the experimental setup and confined geometry target can be found elsewhere.[38]

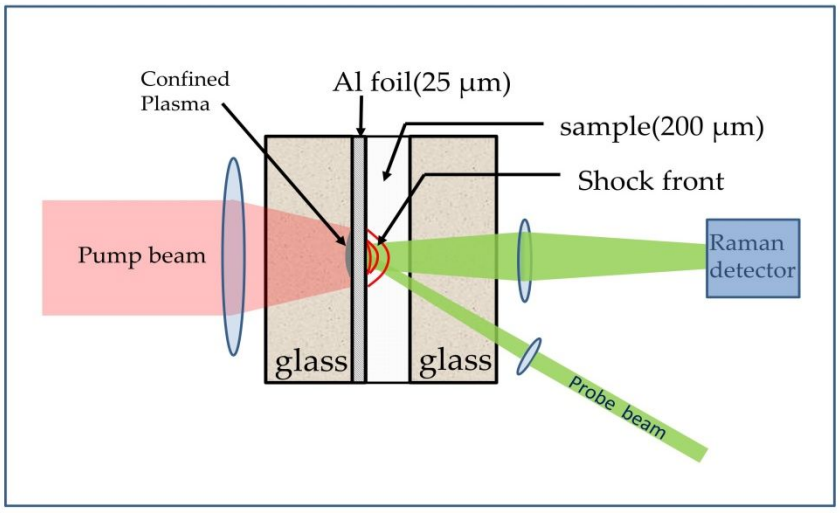


**Fig 1**. Schematic of pump-probe arrangement for the time resolved Raman spectroscopy of shocked medium. Pump beam hit the target at normal, however, the probe beam hits at $45^0$ which enable the efficient collection of scattered Raman signal.

**B: Raman spectroscopy under Static compression**

*In-situ* Raman spectra of benzene were recorded using a confocal micro-Raman spectrograph (JobinYvonT6400) in single stage mode. A 532 nm diode pumped solid state laser was used as an excitation source for these experiments. A 20× objective lens was used to collect the Raman scattered signal in backscattering geometry. The high-pressure was generated using a modified symmetric type of diamond anvil cell equipped with diamond anvils of ~ 300 μm culet. The volatile benzene in liquid form was carefully loaded along with a speck of ruby as a pressure marker into the sample chamber (~100 μm diameter) which is made of a hardened stainless steel gasket pre-indented to a thickness of ~60 μm. The pressure is measured using the ruby fluorescence technique [39] using equation.

$$P(GPa) = 380.8\left[\left(\frac{\lambda}{\lambda_0}\right)^5 - 1\right] \qquad (1)$$

Where, $\lambda$ is measured wavelength of the ruby $R_1$ line and $\lambda_0$ = 694.24 nm is the zero-pressure value at 298 K. In this study we have carried out static Raman spectroscopic measurements up to 15 GPa, (although our capability is up to Mbar pressures) to compare with the shock wave data. The maximum pressure achieved in shock experiment is limited by damage threshold of glass used in confinement geometry and is 5 GPa in Benzene.

### C: Radiation-Hydrodynamics Simulations

Since the Raman signal recorded is a result of contributions from variously shocked and unshocked regions of the target, it becomes pertinent to try and account for these various contributions in the interpretation. To help validate our observations we performed numerical simulation using the HYADES code which is a one-dimensional, three-temperature Lagrangian Radiation-Hydrodynamics simulation code.[40] The code was used to estimate the peak pressures achieved at each laser intensity and to otherwise inform the analysis. The simulation region consisted of four zones: 500 µm of glass, 25 µm of Al, 200 µm of benzene and then a further 500 µm of glass. Accurately simulating the full thickness of the glass at the front and rear of the target was deemed unnecessary given that it is not expected that the outermost regions of the glass layers would play any role in the shock-physics. The pump laser profile was matched to that used in the experiment. Radiation transport was handled using a multi-group radiation diffusion approximation with 40 groups. Electron conduction was modelled using a flux-limited diffusion scheme and SESAME equation of state (EOS) tables were employed for the Al and glass layers. No benzene table was available. Ionization was modelled using an average-atom LTE approximation.

## Results & Discussion:

## Raman Studies with varying strength of shock compression

High-resolution Raman spectra of the C-C ring breathing mode ($\nu_1$) of benzene at 995 $cm^{-1}$ (our spectrometer is offset by 2 $cm^{-1}$ compared to spectrometer used in the static compression measurement) are measured at various dynamic pressures (1.3-4.6 GPa) by varying the pump energy from 100-1300 mJ (0.49 GW/$cm^2$ to 6.4 GW/$cm^2$) and keeping the optical delay fixed at 52 ns. Our spectrum is slightly different from the earlier published data





For Peer Review

due to the higher resolution. In earlier published work with 600 /1200 lines per mm groove-density grating, a single broadened peak, a combination of Raman modes generated from shocked and unshocked regions, is usually observed due to the lower spectral resolution. Our experiments have been performed with a higher grove-density grating (2400 lines /mm). Hence, Raman spectra with well resolved peaks are observed as shown in figure 2a. Since the Raman probe beam interacts with the entire depth of sample, the spectrum obtained is a combination of signal obtained from the unshocked (first peak) and shocked regions of the sample (second broad peak). On careful analysis, it is observed that the multiple peaks are emerging due to scattering from different pressure region of the sample in contrast to the earlier reported work where signals could only be attributed to two regions namely unshocked and shocked assuming constant shock pressure throughout the sample. To understand the behaviour observed in the present high-resolution experiment we performed numerical simulations at various laser intensities corresponding to our experimental intensities. In order to extract the multiple peaks from the signals emerging from shocked and unshocked regions, we have deconvoluted the signals using multiple Lorentzian curve fitting. For comparison, the experimental Raman spectra and the simulated spatial profile of shock wave at a delay time of 52 ns for different pressures are shown in Fig 2 a & b. From 1.3 to 3.1 GPa the experimental Raman spectra is fitted with three Lorentzian peaks: one from the unshocked region and other two from the shocked region (shown in cyan & orange). Under shock compression the $\upsilon_1$ mode shows new peak due to phase II in addition to the pressure induced blue shifted Raman peak corresponding to phase I at lower pressure i.e., 1.3 GPa while under static compression it is observed at 2.3 GPa. This phase transition at lower pressure in the case of dynamic compression may be due to the shock temperature. This agrees with the phase transition at 1.4 GPa reported by Theiry et al.[23] for annealed benzene held at 373 K for 24 hours in the DAC prior to measurement. They also reported that at room temperature the phase transition occurs at ~ 2.5 GPa, similar to our static pressure measurement in which, this phase transition is observed at 2.3 GPa. Schmidt et al. [35] in their backward stimulated Raman Scattering studies under shock compression up to 1.2 GPa have reported a comparative study of their dynamic compression data with high temperature static compression data of liquid benzene. The ring stretching Raman mode frequency show equal Raman shifts for both the liquid phase and benzene phase II at high temperature static Raman experiments in agreement with their wave number shift for dynamic compression experiments. This led them to the conclusion that at 1.2 GPa under shock compression benzene must have undergone direct transition to Phase II or is in liquid Phase at high temperature due to shock temperature. However, in our high spectral resolution





For Peer Review

measurements, we clearly observed co-existence of both the phases (i.e., Benzene phase I which is orthorhombic and Benzene phase II which is monoclinic) which is similar to results from our static pressure measurements except that it occurs at low pressure i.e. at 1.3 GPa in case of laser shock experiments. In another work, Michael Baggen et al.[41] have shown a phase transition at 1.5 GPa in static compression in a DAC using time-resolved Stimulated Raman Scattering.

On further increase of pressure above 3.1 GPa, new Raman modes starts appearing near to the primary Raman mode shown by blue and green curve in Fig 2a. These new peaks corresponds to the signal scattered from gradient region which is at lower pressure than the peak shock pressure. This gradient in the pressure profile is due to the generation of rarefaction wave after the end of high-power laser pulse. It can also be seen from the simulated spatial profile of shock wave that above 3.1 GPa pressure where pressure profile can be divided into three zones (I, II, & III) marked in graph 2b. Region I show the location of the Al pusher and ablated plasma at 52 ns with respect to the foot of the pump beam arriving at the Aluminium foil. Region II sits in the benzene and is a region in which the pressure ramps up toward the most recently shocked material. Region III immediately follows the shock wave and has a relatively flat pressure profile. So, in the experiments above 3.1 GPa, two distinct shocked regions are clearly observed (gradient region and flat region). Hence, above 3.1 GPa, we have used four-peak fitting. Two broad peaks are observed from the gradient region (shown in blue &green) as the lowest pressure in gradient region is > 1.3 GPa and two narrow peaks of relatively small amplitude (shown in cyan & orange) due to scattering from the flat region (which is smaller than the gradient region). However, at lower pressure (below 3.1 GPa) region III becomes indistinguishable from region II and hence, other than the peak corresponding to the unshocked material, only two broad shifted peaks are observed due to the continuously varying pressure behind the shock wave. These two peaks are due to formation of new peak in addition to the pressure induced blue shifted Raman mode $\nu_1$ at 992 $cm^{-1}$ due to pressure > 1.3 GPa at which phase transition occurs.

For Peer Review

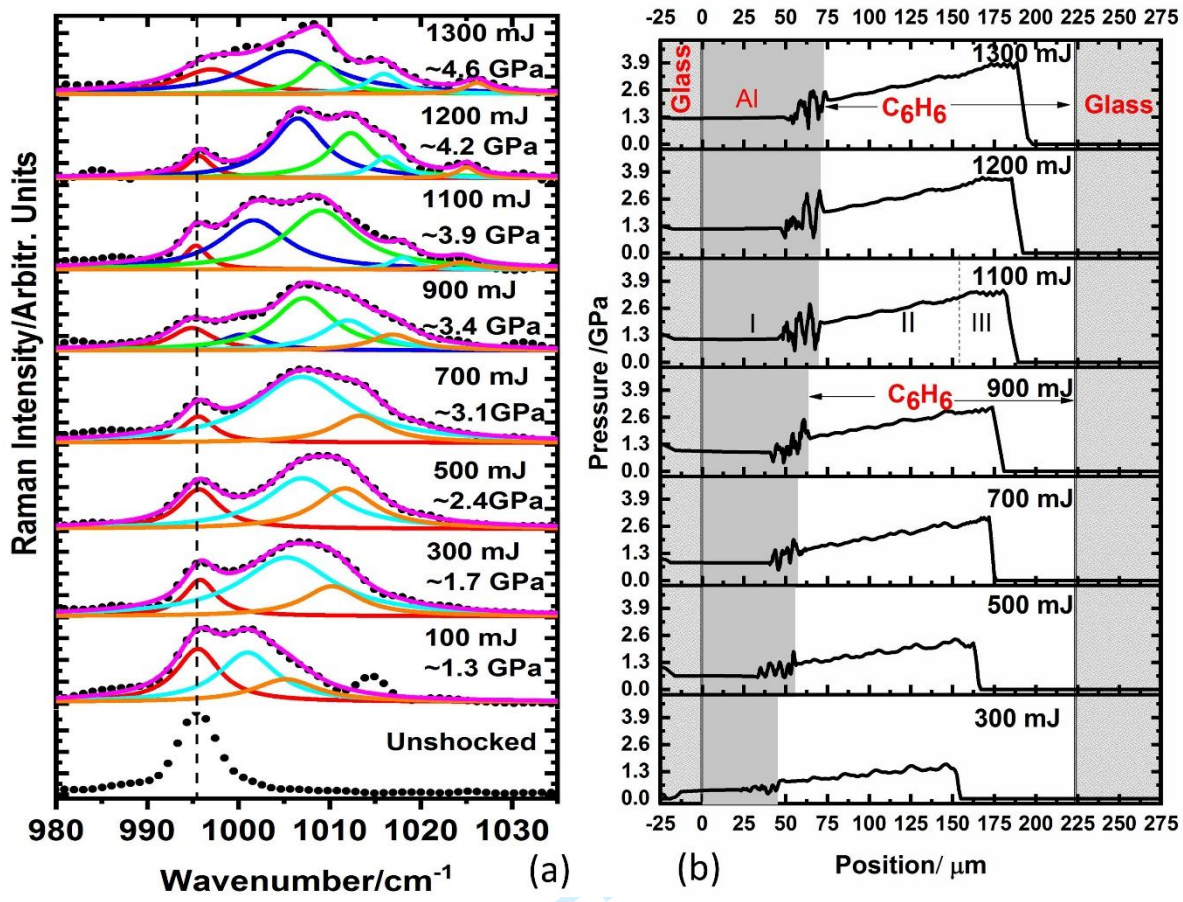


**Fig 2a.** Lorentzian fit of shocked $\nu_1$ (993 cm$^{-1}$) C-C ring breathing mode for different pressures (or laser energies), **b.** Pressure profile at different laser energies for at 52 ns relative to the start of the pump pulse.

## Static Compression Measurements:

At ambient pressure the C-C ring breathing mode ($\nu_1$) of benzene is observed at 993 cm$^{-1}$. Fig. 3a shows the evolution of the Raman mode with increasing pressure. Under compression an abrupt increase in absolute Raman intensity and narrowing of width are observed at 0.3 GPa which indicates that the benzene has undergone the liquid to solid (Phase I) transition.[41] In literature, this transition is at 0.07 GPa, however, our lowest measured static pressure is 0.3 GPa at which benzene is already transformed in its solid form i.e. Phase I having orthorhombic Pbca ($D_{2h}^{15}$) crystal structure with four molecules per unit cell.[42] On further compression up to 2.3 GPa the $\nu_1$ Raman mode blue shifts with slightly decreasing intensity. At 2.3 GPa a new Raman mode arises at ~1009 cm$^{-1}$ near the Raman mode $\upsilon_1$ with a separation of approximately 4.4 cm$^{-1}$. The intensity of this Raman mode increases with pressure. The appearance of a new Raman mode at ~1009 cm$^{-1}$ shows the occurrence of the phase transition

from phase I to phase II in the benzene. The Raman mode at lower frequency i.e., at 1004 $cm^{-1}$ belongs to phase I, while the one at higher frequency i.e., at 1009 $cm^{-1}$ belongs to phase II. The coexistence of these two phases implies a first order phase-transition. G. J. Piermarini et al.[43] reported at room temperature and 1.4 GPa the transition to phase II occurs. The structure of this phase, indicated to be stable up to 4 GPa, was determined by single-crystal x-ray diffraction experiments as monoclinic $P2_1/c$ ($C_{2h}^5$) with two molecules per unit cell. Thiery et al.[23] have also performed XRD experiments on Benzene and observed a similar phase transition at 2.5 GPa in unannealed benzene and concluded that the phase transition pressure reported by Piermarini et al is an inaccurate pressure determination[43] to assign to phase II for unannealed sample. This transition pressure is higher than the shock transition pressure which is 1.3 GPa and to the earlier reported studies by Thiery et al.[23] who had reported this transition to occur above 1.4 GPa for annealed benzene in static compression using Raman and XRD studies. Schmidt et. al.[35] has also observed that under static compression at temperature ~ 200 $^0$C, Phase -II occurs at about 1.2 GPa. Ciabini et al.[44] reported using IR spectroscopy and ADXRD that in the annealed sample only the two expected crystal components for a monoclinic cell with two molecules in the unit cell are observed, even though partly overlapped. On the contrary, a triplet is observed in the unannealed sample indicating the coexistence of the orthorhombic to which the two low frequency bands belong and monoclinic phases revealed by the higher-frequency band. In our Raman spectroscopic studies using static compression of normal benzene at room temperature, we too observed both the phases i.e., phase I and phase II are also found to coexist above 2.3 GPa in the unannealed benzene sample up to the highest measured pressure of 14.3 GPa. However, the intensity of new Raman mode increases at the cost of $\nu_1$ until it becomes comparable at 7.3 GPa (see figure 3a). At pressure 14.3 GPa the intensity of the new Raman mode becomes three times that of the Raman mode at corresponding to phase I. This again confirms the sluggish nature of this phase transition even up to 14.3 GPa. It is concluded from above discussion that in unannealed benzene the phase transition from Phase I to Phase II is very sluggish in nature and it requires thermal activation for complete transformation from phase I to phase II and same has also been pointed out by Thiery et. al. [23] The peak position as a function of pressure is plotted in Fig. 3b. For phase I the slope dv/dP of Raman mode at ~ 993 $cm^{-1}$ is 5.1 $cm^{-1}$/ GPa which is comparable with its earlier reported value as 5.0 $cm^{-1}$/ GPa by Theiry et. al.[23] At higher pressure > 2.5 GPa, the slope for the two Raman modes at 1004 $cm^{-1}$ and 1009 $cm^{-1}$ are 3.1 $cm^{-1}$ / GPa and 3.8 $cm^{-1}$/ GPa respectively. Weizhao et. al.[34] observed slope of 4.32 $cm^{-1}$/GPa for pressure





For Peer Review

lower than 4.2 GPa (Benzene-I) and above this pressure 2.61 $cm^{-1}$/GPa & 3.25 $cm^{-1}$/GPa for the two modes of Benzene in phase-I and –II in their static experiments[34] Baggen et. al.[41] observed a phase change from Benzene -I to Benzene -II at 1.5 GPa in static experiments and observed slope of 4.6 $cm^{-1}$/GPa for lower than this pressure. Above this phase transition pressure slopes are 4.1 $cm^{-1}$/GPa and 4.4 $cm^{-1}$/GPa for the Raman modes in phase I & II respectively. Considering all these experimental data, it was observed that the Benzene-I to Benzene-II phase transitions occurred between 1.3 to 4.2 GPa depending on the experimental conditions and further reported that the second phase transition is sluggish in nature i.e., both phases Benzene-I & II coexist up to higher pressure.

Our experimental data are plotted in figure 3b along with the data taken from Thiery et al.[23], Schmidt et al.[35], Baggen et al.[41], Hiller et al.[45] and Weizho et al.[34] From figure 3b it is clear that our experimental data is in close agreement with the Raman data from Thiery et al.[23] Apart from this it matches well with the other researchers' data also.

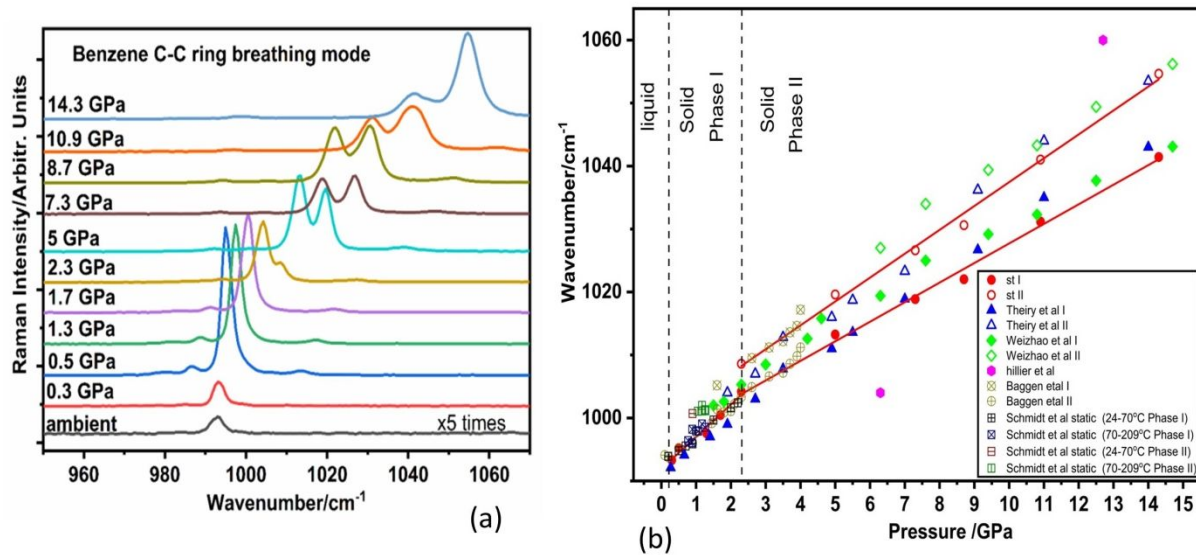


**Fig 3(a).** Stacked plot of Raman spectra of the C-C ring breathing mode ($\nu_1$) of benzene (993 $cm^{-1}$) under Static compression at different pressures. Spectra at ambient is scaled five times. **(b)** Data from our static pressure measurements are shown as closed and open red circle for Phase -I and phase-II respectively. St-I and St -II indicates the Raman modes in Phase I and II under static compression. Red lines are linear fit to the data for guiding eyes. For other's data, I & II marked against their name are correspond to phase-I and phase-II.

Fig 4 shows comparison of the Raman shift obtained under static and shock compression conditions. In this figure, the shock pressure amplitude is taken from the

simulation for the respective pump laser energy on target. The validity of the shock pressure generated by simulation was validated by the experiment using time resolved measurement which will be discussed in more detailed in the next section. The simulated pressure is about 8 % lower than the estimated pressure from the time resolved measurement. It can be seen from this figure that the Raman mode shift in the case of dynamic compression is higher than that in static pressure in the same pressure range, which is not very obvious, since, static compression is isothermal and hence should produce greater compression than a shock of equivalent pressure. Also, the phase transition from phase I to Phase II occurs at 1.3 GPa in dynamic compression is occurred rather than 2.3 GPa as in case of static compression experiment. However, Schmidt et al. [35] have also showed a higher shift in the case of gas-gun driven dynamic compression experiments as compared to those seen via static compression studies. They have also shown that the Raman mode shift for the dynamic experiments agrees well with their high temperature static compression data for either liquid Benzene or Benzene-II. At pressures below I-II-Liquid triple point pressure i.e., 1.2 GPa, the shocked Benzene is probably at temperatures high enough for it to be in liquid state. This indicates that Schmidt et. al.[35] observed higher Raman shift than their static compression experiments and mentioned that it may be due to phase transition from liquid to phase-II of Benzene or liquid Benzene at higher temperature. However, they could not identify the existence of phase-I due to poor resolution of the spectrograph. In our measurement with high resolution spectrometer, we clearly identify that at pressure 1.3 GPa and higher, both phases i.e., Benzene-I and Benzene -II coexists similar to our static pressure measurement in which both phases coexist for full range of our measurement. There may also be a possibility that below this pressure there is a phase transition from liquid Benzene to solid Benzene-I like our static pressure measurement, where we notice a liquid to solid phase transition at 0.3 GPa. However, in our shock experiment the lowest pressure, measured using laser is 1.3 GPa. With above discussions, we can say that that in case of dynamic compression experiments using lasers, there may be two phase transitions (Liquid-solid Benzene-I & Benzene-I to Benzene-II) similar to static one except the difference of phase transition pressure from Benzene-I to Benzene-II which is lower in our dynamic experiments. Figure 4 represents the comparison of our dynamic compression experimental data with our static compression data along with others static and shock compression results. St-I, St-II and Sh-I, Sh-II represents data points of the present work corresponds to the Benzene-I and Benzene-II measured in static and dynamic (Shock) experiments respectively. Shock gradient I and Shock Gradient II represents the two new modes from gradient region II in Fig 4. Works from other authors in Benzene phase I and benzene phase II are represented by I and II in front



For Peer Review

of the author names. The results of Matsuda et al [15,46,47] in solid phase are in close agreement with our Sh-I data while the data of Matsuda et al in liquid phase match with our Sh II data points.

We have also studied the effect of reflected shock wave from benzene-glass interface into the pre-compressed benzene sample by forward moving shock wave. For this purpose, we have extended delay between pump and probe beams till 108 ns in our time resolved measurement for a fixed 700 mJ laser energy which is discussed in the next section. This delay is good enough to see the reflected shock wave movement throughout the benzene sample.

From the experimental data it is seen that the shock wave reached to the benzene -glass interface somewhere between 63-65 ns as two new peaks are observed at higher wave number in the spectra recorded for delay of 66 ns and above. These two peaks (1015 $cm^{-1}$ & 1022 $cm^{-1}$) corresponds to Benzene-I and Benzene-II at higher pressure due to reflected shock. However, our simulation shows that the shock reaches to interface at 71 ns. These peaks at higher wave number correspond to the pressure of approximately 5 GPa and the same pressure can be seen from simulation in the reflected shock wave but at somewhat later times. The reflected pressure is 1.64 times that of the forward moving pressure (3 GPa @ 700 mJ) incident at the benzene-glass interface. This degree of pressure increase agrees with the results of an impedance mismatch calculation [48]:

$$P_2/P_1 = 2\rho_{0glass}\, C_{0glass}/(\rho_{0benzene}\, C_{0benzene} + \rho_{0glass}\, C_{0glass}) = 1.8 \qquad (2)$$

Where $P_2$ is the reflected and $P_1$ is incident shock pressure at the Benzene-glass interface, $\rho_0$ is the density of at room temperature and pressure, $C_0$ is the speed of sound in the medium. The subscripts Benzene and glass means the density and sound speed in respective medium. In Fig 4, the peaks of the modes shifts due to the reflected shock pressure are represented by star symbols (Green and red) due to coexistence of Benzene-I and Benzene-II at 5 GPa. The (star symbols) i.e., mode shifts are slightly higher than the peaks generated by the forward going shock wave and of similar amplitude. This high shift may be due the reason that the reflected shock is moving in the pre-compressed medium which will be at higher pressure and temperature than the normal benzene sample. It can be seen from the simulation that at larger time delays, as the reflected shock wave travels further back into the sample that its amplitude decreases as it propagates into material at increasingly low density. For example at 81 ns delay the sample is divided into two pressures i.e. 3.6 GPa and 1.2 GPa and



For Peer Review

corresponding peak shifts towards lower wave number side and corresponding mode shifts are at 1013 $cm^{-1}$, 1016.2 $cm^{-1}$ and 998.7 $cm^{-1}$ and 1004.1 $cm^{-1}$ respectively. On further delay if 94 ns, the reflected shock has moved more than half of the sample and pressure reduced to 2.5 GPa and 0.8 GPa and the corresponding mode shifts are 1008.7, 1014 $cm^{-1}$ for Benzene-I and Benzene-II respectively and since 0.8 GPa is lower than 1.3 GPa (phase transition pressure) only single peak corresponding to this pressures is observed at 999.7 $cm^{-1}$. Finally, at 108 ns delay, the reflected shock wave has traversed almost ¾ part of the sample and the reflected shock pressure and the remaining pressure due to forward moving shock waves are 2 GPa and 0.6 GPa corresponding to shifts of 1007 $cm^{-1}$, 1012 $cm^{-1}$ & 996.9 $cm^{-1}$. This correlates to the experimental observation that the amplitude of the associated peaks are increasing and shifting to lower frequencies. This effect is illustrated with dotted lines in figure 5a with the corresponding simulated pressure profiles in figure 5b. So, from our measurement we conclude that, there are two phase transitions one Liquid to Solid Benzene -I and Benzene-I to Benzene-II at < 1 GPa and 1.3 GPa respectively due to laser driven shock wave in Benzene sample.

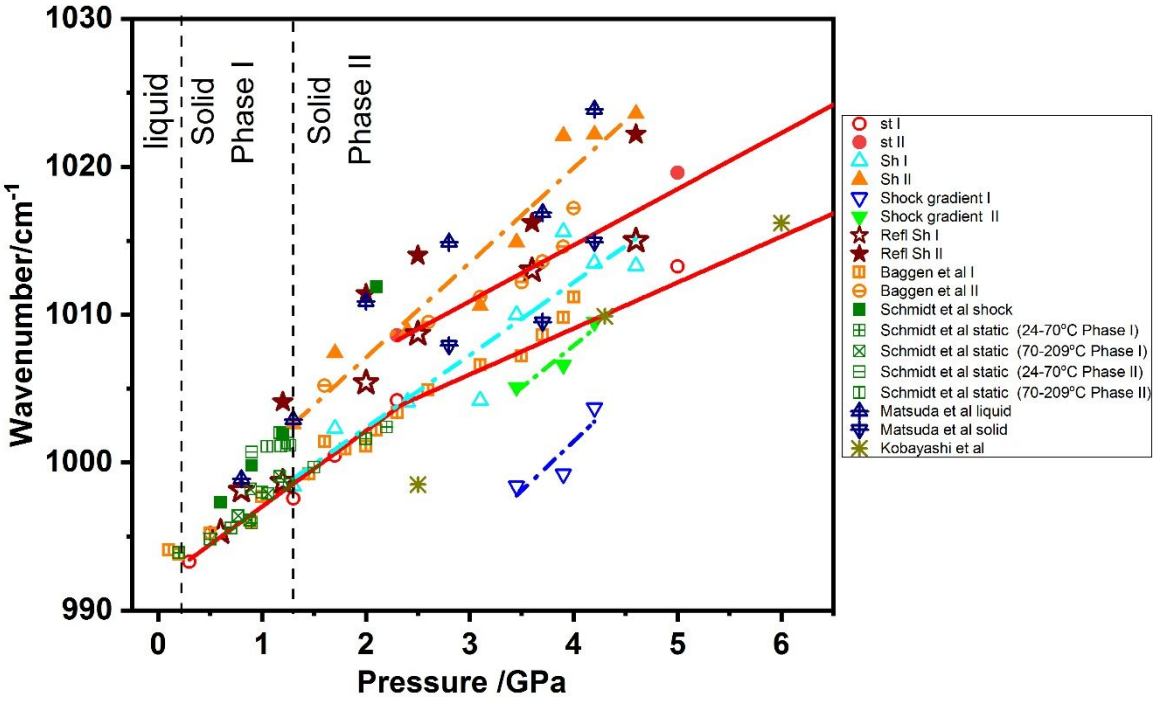


**Fig 4** Comparison of Raman shift obtained under shock and static compression (Solid lines are a linear fit to the static compression data; dotted lines are a fit to the shock compression data). St-I, St-II and Sh-I, Sh-II represents data points of the present work corresponds to the Benzene-I and Benzene-II measured in static and dynamic (Shock) experiments respectively.

Shock gradient I and Shock Gradient II represents the two new modes from gradient region II. Ref Sh I and Ref Sh II represent the mode shift due to reflected shock wave in the present studies. Works from other authors in Benzene phase I and benzene phase II are represented by I and II in front of the author names.

## Raman Studies with varying delay time:

Figure 5a shows the stacked plot of time-resolved Raman spectra of the C-C ring breathing mode of benzene (995 $cm^{-1}$) under laser-driven shock compression at different delay times from 9 ns to 108 ns for a fixed laser energy of 700 mJ. The black curve represents the Raman spectra under ambient conditions and the red curve represents the Raman spectra under shocked conditions. From the spectra obtained at 9 ns it can be seen that the Raman spectra is similar to that obtained in ambient conditions hence it can be inferred that the shock has not yet entered the sample and is still in aluminium in agreement with the simulation. As the time progresses to a delay of 17 ns, a new pressure induced peak is observed at a higher wave number in addition to the ambient peak. Hence, it can be assumed that the shock has entered the sample by 17 ns and the new peak is due to benzene molecules under shock compression. We observed three peaks in shocked conditions at 31 ns, one from the unshocked region and other two from shocked region one due to shock induced blue shifted fundamental and other due to formation of new phase (Benzene-II) at this pressure. For the higher delays from 45-59 ns an additional two peaks at lower wave number are observed which are from the lower pressure gradient region (ramped part) of the shocked sample (region II). This gradient pressure is due onset of rarefaction wave in the sample once the laser pulse is over. Hence, a total of five Lorentzian peaks were fitted one from the unshocked region (red), two from flat shocked region III (shown in cyan and orange) and other two (blue and green) due to the pressure gradient region II. At increased delays, a larger sample volume is under shock compression and hence the intensity of the peak from unshocked region decreases as can be seen at delays of 45, 52 & 59 ns. At higher delay times the intensity of the blue and green peaks are observed to be increasing till 66 ns, which is due to the increased volume occupied by this gradient region at larger time delays. These blue and green coloured peak's intensities start decreasing for delay more than 66 ns to 80 ns and peak also shifted towards shorter wave number. Here two peaks is due to pressure more than 1.3 GPa in the gradient region. However, for delay 94 ns and 108 ns, the gradient region pressure is less than 1.3 GPa and hence only one peak is available (blue

For Peer Review

colour) from Benzene-I and same can be seen from simulation output shown in figure 5b. The fast decrease in shock amplitude of gradient region and reflected shocked regions are due to interaction of reflected shock and rarefaction wave which makes drastic decrease in the shock profile.

Now, for shock velocity measurement we will concentrate for the delay between 9 – 66 ns. At 66 ns it is observed that the intensity for the peak corresponding to unshocked region is almost nil, however, two new peaks (orange and dark yellow) at higher wave number seems to be emerging. From this observation, it seems that by 66 ns the shock must have traversed the whole sample and these new peaks are attributed to the modes emerging from coexistence of Benzene-I and Benzene-II due to reflected shock wave at 5 GPa which has already been discussed in previous section. This indicates that the shock wave must have reached the interface in 63-65 ns corresponding to a shock velocity of approximately 3.57 ± 0.3 km/s. However, our simulation shows shock velocity of approximately 3.3 km/s (corresponding to a shock travel time through sample of 71 ns) and a shock pressure of about 3.1 GPa. From 66 ns onwards the orange and dark yellow curves represent the reflected shock. These peaks are shown in Fig 4 as Ref Sh I and Ref Sh II by star symbols. It can be observed that the intensity of this peak increases with time while its peak shifts towards lower wave number. This intensity increase is due to the increased volume of the twice-shocked (reflected shock) material while the shift towards lower wavenumber is due to the rapid decay in reflected shock pressure with time due to the interaction of reflected shock wave with rarefaction wave. This effect is also observed in the numerical simulations. While the simulations and experiments agree well overall, it is thought that the disagreement in the shock wave transit time through the benzene is most likely a consequence of the benzene EOS being poorly represented in the simulation. (The fact that the simulations are 1D would tend to produce an error in the opposite direction to that observed).

To validate our results we also calculated the shock velocity by evaluating the temporal evolution of intensity ratio of shocked to total original peak intensity at a fixed laser energy of 700 mJ based on the formula given in ref [49]. The shock velocity $U_s = r.t$, where r is estimated from the temporal evolution of ratio of intensity of shocked to total original peak intensity and t is target thickness. Fig 6a shows the plot of evolution of intensity ratio with delay time of 7 to 80 ns. Here, it can be seen that the plot is flatten after 66 ns as after this delay no unshocked region is available. The slope of plot is (0.018 ±0.002) x $10^9$ $s^{-1}$ (if 59 ns considered as exit



For Peer Review

time). Since we do not have delay adjustment less than 7 ns, so there is no data in between 59 to 66 ns. The shock velocity estimated from experimental intensity ratio is 3.6 ±0.4 km/s which is close to the velocity 3.57 ± 0.3 km/s calculated based on the Raman signal (experimental data) at 66 ns. This also indicates that the shock traverse time lies between 63-65 ns. Since, this experiment is very expensive due to the destructive nature of shock wave, we have measured time evolution of the Raman peaks at only one energy i.e. 700 mJ. However, we performed simulations at pump energies ranging from 100 mJ to 1300 mJ used in the experiments. The shock velocity obtained from simulation at 700 mJ is 3.3 km/s (considering 71 ns as exit time). Shock velocities extracted from simulation for all energies are plotted and compared with the experimental shock velocity measurement at 700 mJ in figure 6b. Our experimental results are within 8 % variation with the simulation results.

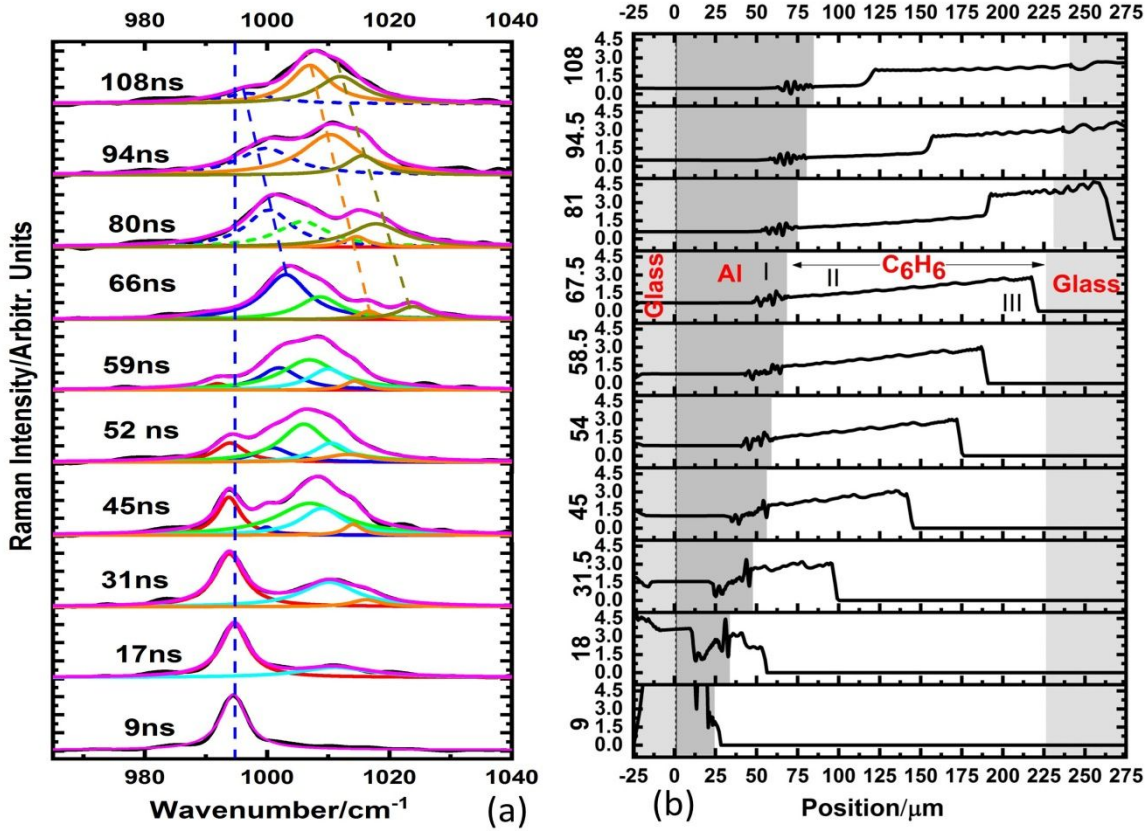


**Fig 5a** Lorentzian fit of shocked $\nu_1$ (992 $cm^{-1}$) C-C ring stretching mode for different delay times, **b.** Spatial profile of Shock wave at different delay times for laser energy of 700 mJ obtained from one dimensional hydrodynamic simulations

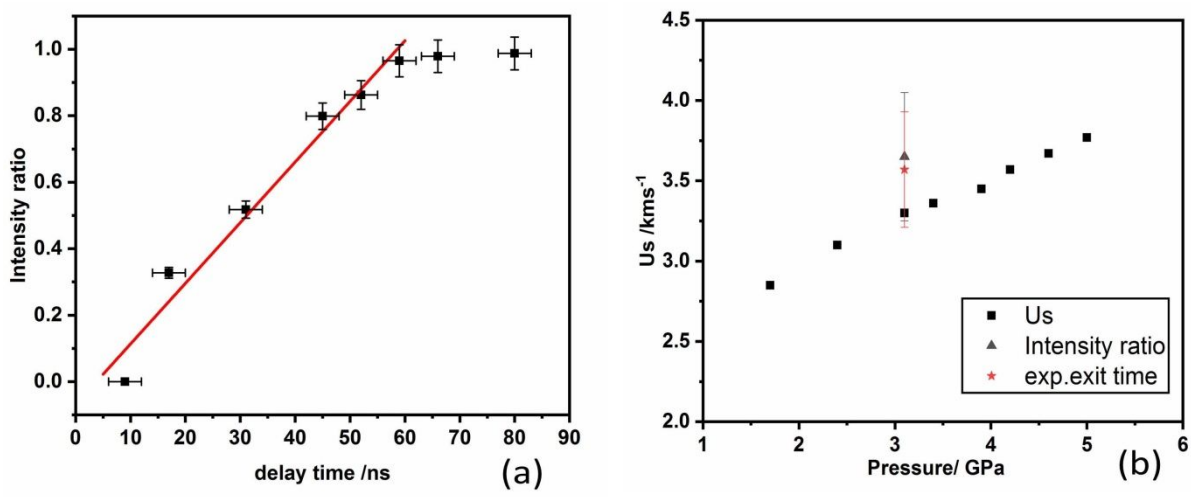


**Fig 6a** Plot of temporal evolution of intensity ratio of $\nu_1$ (993 $cm^{-1}$) C-C ring breathing mode with delay between pump and probe beams. **(b)** Comparison of the shock velocity deduced from the simulation versus that calculated using intensity ratios of the Raman signal from the shocked region to the total region and based on the appearance of a new Raman peak and the disappearance of the peak corresponding to the unshocked region at 66 ns indicating that the shock has traversed the entirety of the benzene sample apart from partly reflection, causing the formation of a new Raman peak.

## Conclusions:

In summary, we have presented our results of high resolution time-resolved Raman spectroscopic experiments performed on laser-driven shock-compressed benzene using confined geometry targets for various delay times as well as for various laser intensities. Experimental results were compared with the static pressure experiments done by us and others in the field. In case of static pressure measurement, we have observed two phase transitions (liquid to solid Benzene and Solid Benzene -I to Solid Benzene – II) at 0.3 and 2.3 GPa respectively. However, in dynamic compression case, Benzene-I (orthorhombic) to Benzene-II (monoclinic) phase transition occurs at 1.3 GPa. No further phase transition is observed till the maximum experimental pressure of 5 GPa in shock experiments. Numerical simulations were performed to estimate the shock pressures. Raman spectra obtained under shock compression showed new pressure induced blue-shifted Raman modes. The high-resolution mode used for these experiments enabled us to study the effects of the pressure gradient produced by the passage of the shock wave upon vibrational properties. The results are corroborated using radiation-hydrodynamics simulations and comparison with static compression measurements. A shock velocity of 3.6 km/s is estimated using the temporal

For Peer Review

evolution of intensity ratios which is within 8% error bar of the simulated results evaluated as 3.3 km/s.

## Acknowledgments:

The authors are also thankful to Mr. Ashutosh Mohan, Mr. D.S. Munda and R.S. Sabale for their technical support and discussions during the performance of the shock-loaded experiments.

## References:

[1]. G. Tas, J. Franken, S. A. Hambir, D. E. Hare, and D. D. Dlott, *Phys. Rev. Lett*. **1997**; 78 (24), 4585.

[2]. Y. M. Gupta, *High Pressure Res*.**1992;** 10 (5-6), 717.

[3]. V. V. Milyavskiy, A. V. Utkin, A. Z. Zhuk, V. V. Yakushev, and V. E. Fortov, *Diamond Relat. Mater*. **2005;** 14 (11), 1920.

[4]. M. Millot, N. Dubrovinskaia, A. Černok, S. Blaha, L. Dubrovinsky, D. G. Braun, P. M. Celliers, G. W. Collins, J. H. Eggert, and R. Jeanloz, *Sci.* **2015 ;** 347 (6220), 418.

[5]. M. Guarguaglini, J. A. Hernandez, T. Okuchi, P. Barroso, A. Benuzzi-Mounaix, M. Bethkenhagen, R. Bolis, E. Brambrink, M. French, Y. Fujimoto, R. Kodama, M. Koenig, F. Lefevre, K. Miyanishi, N. Ozaki, R. Redmer, T. Sano, Y. Umeda, T. Vinci, and A. Ravasio, *Sci. Rep.* **2019;** 9 (1), 10155.

[6]. S. K. Atreya, P. R. Mahaffy, H. B. Niemann, M. H. Wong, and T. C. Owen, *Sci.* **2003;** 51(2), 105.

[7]. Z. A. Dreger, and Y. M. Gupta, *J. Phys. Chem. B* **2007**; 111(15), 3893.

[8]. N. Hemmi, Z. A. Dreger, Y. A. Gruzdkov, J. M. Winey, and Y. M. Gupta, *J. Phys. Chem. B* **2006**; 110 (42), 20948 .

[9]. F. Garcia, K. S. Vandersall, and C. M. Tarver, *J. Phys.: Conf. Ser.* **2014**; 500 (5), 052048.

[10]. Kozu, T. Kadono, R. I. Hiyoshi, J. Nakamura, M. Arai, M. Tamura, and M. Yoshida, Propellants, *Explos. Pyrotech.* 2**002**; 27(6), 336.

[11]. A. P. Pogorelov, and S. A. Novikov, *Combust. Explos. Shock Waves* **1985**; 21(4), 496.

[12]. C. Saint-Amans, P. Hébert, M. Doucet, and T. de Resseguier, *J. Appl. Phys.* **2015**; 117(2), 023102.

[13]. R. Sivaramakrishnan, K. Brezinsky, H. Vasudevan & R. S. Tranter, *Combust. Sci. Technol.* **2006**; 178 , 285.

[14]. T. S. Duffy, R. F. Smith , *Front. Earth Sci.* **2019**; 7, 23.

For Peer Review

[15]. D. D. Dlott, *Annu. Rev. Phys. Chem.* **1999**; 50(1), 251.

[16]. A. Matsuda, & K.G. Nakamura, & K. I. Kondo, *Phys. Rev. B* **2002**; 65, 174116.

[17]. K. G. Nakamura, K. Wakabayashi, A. Matsuda, and K. I. Kondo, *Appl. Surf. Sci*. **2002**; 197, 17.

[18]. J. Akella, and G. C. Kennedy, *J. Chem. Phys.* **1971**; 55(2), 793.

[19]. W. D. Ellenson, and M. Nicol, *J. Chem. Phys.* **1974**; 61(4), 1380.

[20]. D. M. Adams and R. Appleby, *J. Chem. Soc., Faraday Trans. 2.* **1905**; 73(7), 1896.

[21]. A Anderson, B Piwowar, W Smith , *Spectrosc. Lett.* **1998**; 31(8), 1811.

[22]. F. D. Medina and D. C. O'Shea, *J. Chem. Phys.* **1977**; 66(5), 1940.

[23]. M. M. Thiery, and J. M. Leger, *J. Chem. Phys.* 1988; 89(7), 4255.

[24]. J. C. Chervin, B. Canny, M. Gauthier, and Ph. Pruzan, *Rev. Sci. Instrum.* **1993**; 64, 203.

[25]. M. Zhou, K. Wang, Z. W. Men, S. Q. Gao, Z. W. Li, C. L. Sun, *Spectrochim. Acta Part A* **2012**; 97, 526.

[26]. X Li-Wen, W Ru-ju, C Liang-chen , *Chin. Phys. Lett.* **1996**; 13(4) 293.

[27]. M Podsiadło, K Jakóbek, A Katrusiak , *Cryst. Eng. Comm.* **2010;** 12(9) 2561.

[28]. A Budzianowski, A Katrusiak, *Acta Crystallogr., Sect. B: Struct. Sci.* **2006;** 62 (1) 94.

[29]. L. Ciabini, M. Santoro, R. Bini, and V. Schettino, *J. Chem. Phys.* **2001**; 115(8), 3742).

[30]. L. Ciabini, M. Santoro, F. A. Gorelli, R. Bini,V. Schettino, and S. Raugei, *Nat. Mater.* **2007**; 6(1), 39.

[31]. M. Pravica, O. G. Urosevic, M. Hu, P. Chow, B. Yulga, and P. Liermann, *J. Phys. Chem. B*. **2007**; 111 (40), 11635.

[32]. Ph. Pruzan, J. C. Chervin, M. M. Thiéry, J. P. Itié, J. M. Besson, J. P. Forgerit, and M. Revault, *J. Chem. Phys.* **1990**; 92, 6910.

[33]. A Katrusiak, M Podsiadło, A. Budzianowski, *Cryst. Growth Des.* **2010;** 10 (8) 3461.

[34]. W. Cai, M. Dunuwille, J. He, T. V. Taylor, J. K. Hinton, M. C. MacLean, J. J. Molaison, A. M dos Santos, S. Sinogeikin, and S Deemyad, *J. Phys. Chem. Lett.*, **2017**; 8(8), 1856.

[35]. S. C. Schmidt, D. S. Moore, D. Schiferl, and J. W. Shaner, *Phys. Rev. Lett.* **1983**; 50(9), 661.

[36]. T. Kobayashi and T. Sekine, *Phys. Rev. B* **2000**;**62**, 5281

[37]. S. Root, Y. M. Gupta, *J. Phys. Chem. A.* **2009;** 113 (7) 1268.

[38]. S. Chaurasia, V. Rastogi, U. Rao, C. D. Sijoy, V. Mishra, and M. N. Deo, *J. Instrum.* **2017**; 12(11), P11008.

[39]. A. D. Chijioke, W. J. Nellis, A. Soldatov, and I. F. Silvera, *J. Appl. Phys*.**2005**; 98(11),114905.

For Peer Review

[40]. HYADES is a commercial product of Cascade Applied Sciences, please contact larsen@casinc.com

[41]. M. Baggen, M. V. Exter, and A. Lagendijk, *J. Chem. Phys.***1987**; 86(4), 2423.

[42]. P. W. Bridgman, *Proc. Am. Acad. Arts Sci.* **1949**; *77*, 129-146.

[43]. G. J. Piermarini, A. D. Mighell, C. E. Weir, and S. Block, *Sci.* **1969**; 165, 1250.

[44]. L. Ciabini, F. A. Gorelli, M. Santoro, R. Bini, V. Schettino, and Mohamed Mezouar, *Phys. Rev. B* **2005**; 72, 094108.

[45]. N. J. Hillier & J. S. Schilling, *High Pressure Res.* **2014**; 34(1),1.

[46]. A. Matsuda, K. Kondo, and K. G. Nakamura, *Jpn. J. Appl. Phys*. **2004**; 43(2), L1614.

[47]. A. Matsuda, K. Kondo, and K. G. Nakamura,*J. Chem. Phys.* **2006**; **124**, 054501.

[48]. S. Eliezer , The interaction of high-power lasers with plasmas, CRC press **2002**.

[49]. X. Zheng, Y. Song, J. Zhao, D. Tan, Y.Yang , C. liu, *Chem. Phys. Lett.* **2010**; 499, 231.

For Peer Review

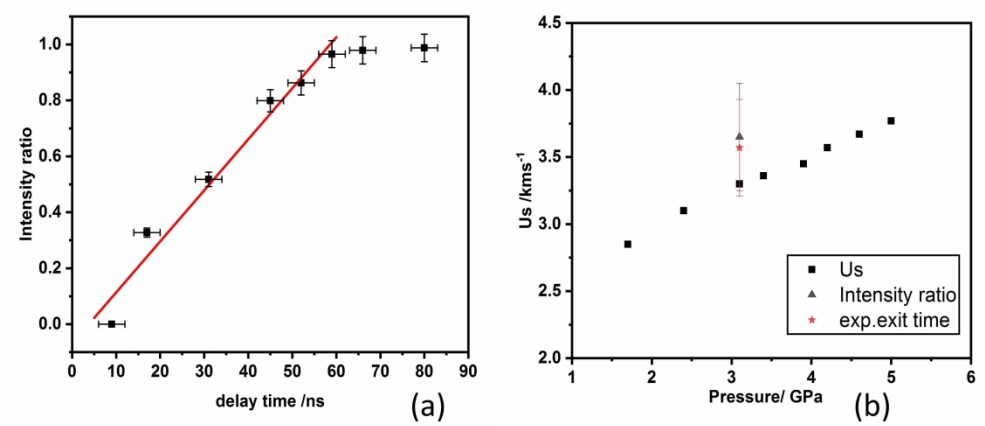


Fig 6a Plot of temporal evolution of intensity ratio of v1 (993 cm-1) C-C ring breathing mode with delay between pump and probe beams. (b) Comparison of the shock velocity deduced from the simulation versus that calculated using intensity ratios of the Raman signal from the shocked region to the total region and based on the appearance of a new Raman peak and the disappearance of the peak corresponding to the unshocked region at 66 ns indicating that the shock has traversed the entirety of the benzene sample apart from partly reflection, causing the formation of a new Raman peak.

254x113mm (300 x 300 DPI)